Published OnlineFirst April 24, 2012; DOI: 10.1158/0008-5472.CAN-11-3135

An NQO1 Substrate with Potent Antitumor Activity That Selectively Kills by PARP1-Induced Programmed Necrosis

Xiumei Huang[1,2], Ying Dong[1,2], Erik A. Bey[1,2], Jessica A. Kilgore[3], Joseph S. Bair[4], Long-Shan Li[1,2], Malina Patel[1,2], Elizabeth I. Parkinson[4], Yiguang Wang[1], Noelle S. Williams[3], Jinming Gao[1], Paul J. Hergenrother[4], and David A. Boothman[1,2]

Abstract

Agents, such as β-lapachone, that target the redox enzyme, NAD(P)H:quinone oxidoreductase 1 (NQO1), to induce programmed necrosis in solid tumors have shown great promise, but more potent tumor-selective compounds are needed. Here, we report that deoxynyboquinone kills a wide spectrum of cancer cells in an NQO1-dependent manner with greater potency than β-lapachone. Deoxynyboquinone lethality relies on NQO1-dependent futile redox cycling that consumes oxygen and generates extensive reactive oxygen species (ROS). Elevated ROS levels cause extensive DNA lesions, PARP1 hyperactivation, and severe NAD^+/ATP depletion that stimulate Ca^{2+}–dependent programmed necrosis, unique to this new class of NQO1 "bioactivated" drugs. Short-term exposure of $NQO1^+$ cells to deoxynyboquinone was sufficient to trigger cell death, although genetically matched $NQO1^-$ cells were unaffected. Moreover, siRNA-mediated NQO1 or PARP1 knockdown spared $NQO1^+$ cells from short-term lethality. Pretreatment of cells with BAPTA-AM (a cytosolic Ca^{2+} chelator) or catalase (enzymatic H_2O_2 scavenger) was sufficient to rescue deoxynyboquinone-induced lethality, as noted with β-lapachone. Investigations *in vivo* showed equivalent antitumor efficacy of deoxynyboquinone to β-lapachone, but at a 6-fold greater potency. PARP1 hyperactivation and dramatic ATP loss were noted in the tumor, but not in the associated normal lung tissue. Our findings offer preclinical proof-of-concept for deoxynyboquinone as a potent chemotherapeutic agent for treatment of a wide spectrum of therapeutically challenging solid tumors, such as pancreatic and lung cancers. *Cancer Res; 72(12); 3038–47. ©2012 AACR.*

Introduction

Lack of selectivity of most cancer chemotherapeutics remains a major limiting factor (1). We have focused on exploiting elevated NAD(P)H:quinone oxidoreductase-1 (NQO1, EC 1.6.99.2) levels in most solid tumors, particularly in non–small cell lung (NSCLC), prostate, pancreatic, and breast (2–4), for drug development. NQO1 is an inducible phase II detoxifying 2-electron oxidoreductase capable of reducing most quinones, forming stable hydroquinones. Glutathione S-transferase then detoxifies hydroquinones, conjugating them with glutathione for secretion (5).

Certain rare compounds, however, may undergo NQO1-mediated bioreduction for antitumor activity. Rather than detoxifying, NQO1 converts specific quinones into highly cytotoxic species. Most antitumor quinones dependent on NQO1 are DNA alkylators: mitomycin C (6, 7), RH1 (8), E09 (7), and AZQ (9). Use of these agents is limited because they are subject to detoxification pathways, efficient substrates for ubiquitously expressed one-electron oxidoreductases that cause normal tissue toxicity, and subject to emergent drug resistance from various DNA repair pathways.

β-Lapachone (Fig. 1A) kills cancer cells and murine xenograft and orthotopic human or mouse tumor models *in vivo* in an NQO1-dependent manner (3, 10). β-Lapachone induces cell death by NQO1-dependent reactive oxygen species (ROS) formation and oxidative stress (2–4). NQO1 metabolizes β-lapachone into an unstable hydroquinone that spontaneously oxidizes, by 2 dioxygen equivalents, generating superoxide (10, 11). Elevated long-lived hydrogen peroxide (H_2O_2) causes extensive DNA base and single-strand break (SSB) lesions that are normally easily and rapidly repaired. However, extensive NQO1-dependent SSBs cause poly(ADP-ribose)polymerase-1 (PARP1) hyperactivation, inhibiting the essential base and SSB repair functions. PARP1 hyperactivation causes dramatic NAD^+/ATP pool losses due to ADP ribosylation, resulting in extensive energy depletion and cell death (2–4). Thus,

Authors' Affiliations: Departments of [1]Pharmacology, [2]Radiation Oncology, and [3]Biochemistry, Simmons Cancer Center, UT Southwestern Medical Center, Dallas, Texas; and [4]Department of Chemistry, Roger Adams Laboratory, University of Illinois at Urbana-Champaign, Urbana, Illinois

Note: Supplementary data for this article are available at Cancer Research Online (http://cancerres.aacrjournals.org/).

X. Huang and Y. Dong contributed equally to this work.

This article is CSCN 066.

Corresponding Authors: Paul J. Hergenrother, Department of Chemistry, Roger Adams Laboratory, University of Illinois at Urbana-Champaign, Urbana, IL 61801. Phone: 217-333-0363; Fax: 217-244-8024; E-mail: hergenro@uiuc.edu; and David A. Boothman, Departments of Pharmacology and Radiation Oncology, Simmons Cancer Center, UT Southwestern Medical Center, Dallas, TX 75390. Phone: 214-645-6371; Fax: 214-645-6347; E-mail: David.Boothman@utsouthwestern.edu

doi: 10.1158/0008-5472.CAN-11-3135

Published OnlineFirst April 24, 2012; DOI: 10.1158/0008-5472.CAN-11-3135

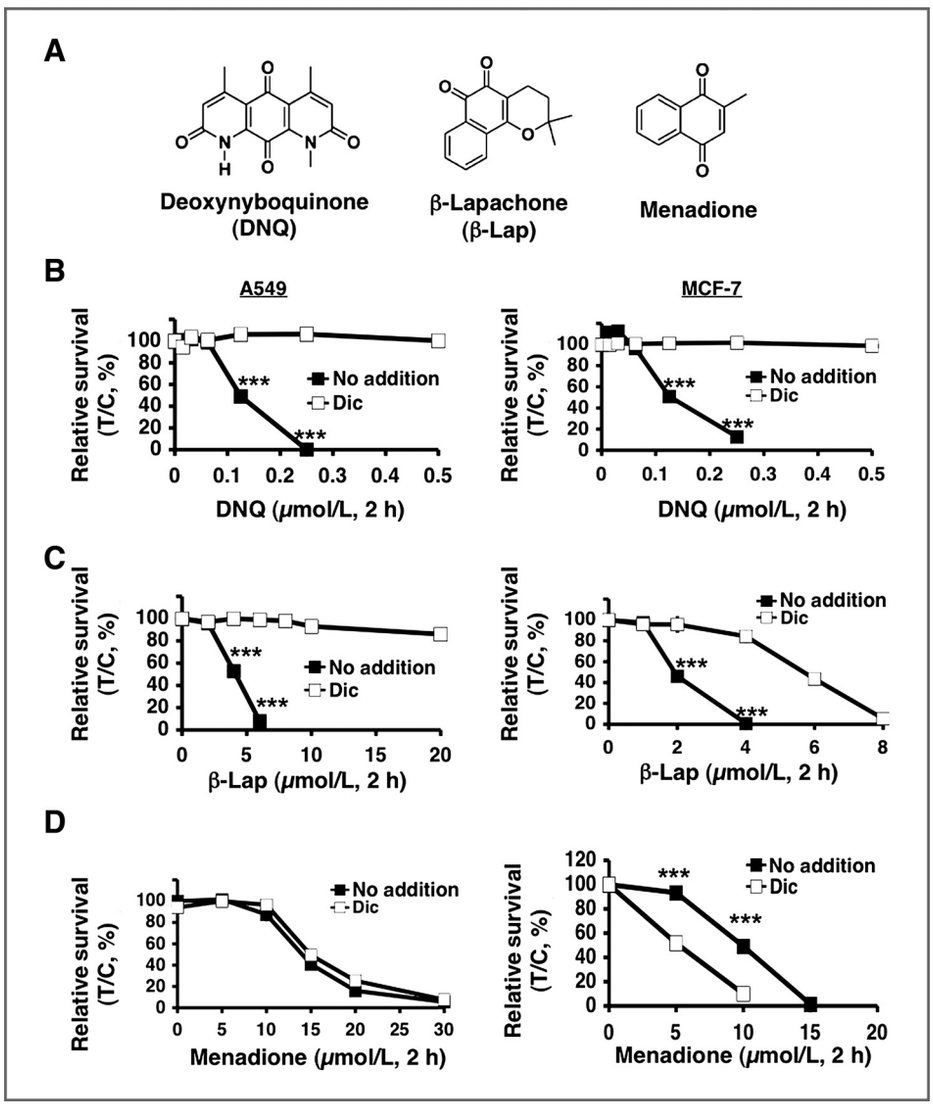

Figure 1. Deoxynyboquinone induced lethality in endogenous NQO1$^+$ cells. A, structures of deoxynyboquinone, β-lapachone, and menadione. B, endogenous, NQO1 overexpressing A549 or MCF-7 cells were treated with or without various deoxynyboquinone doses (μmol/L, 2 hours), ± dicoumarol (40 μmol/L, 2 hours). Lethality was monitored by relative survival. Data are means, ±SE for sextuplets carried out thrice. C, cells from B were treated with or without various β-lapachone doses (μmol/L, 2 hours), ± dicoumarol. D, cells were treated with or without menadione (μmol/L, 2 hours), ± dicoumarol as in B. Dicoumarol potentiated menadione toxicity in MCF-7, but not in A549, cells. Control cells in B–D were treated with identical DMSO concentrations (<0.05%). ***, $P \leq 0.001$. Dic, dicoumarol; DNQ, deoxynyboquinone; β-lap, β-lapachone.

β-lapachone kills NQO1$^+$ cancer cells by programmed necrosis that is independent of caspase activation or p53 status, independent of bcl-2 levels, not affected by BAX/BAK deficiencies, independent of EGF receptor, Ras, or other constitutive signal transduction activation, and/or not dependent on proliferation. β-Lapachone is, therefore, an attractive experimental drug, and various β-lapachone formulations have been, or are in, phase I/II clinical trials.

However, β-lapachone has a modest potency (LD_{50}: 2–10 μmol/L) *in vitro*, with limited aqueous solubility that complicates formulation and delivery. Although nanoparticle strategies for β-lapachone delivery solved formulation issues, resulting in dramatic antitumor efficacy (12), there is a clear need for higher potency drugs.

Deoxynyboquinone (Fig. 1A) is a promising antineoplastic agent whose mechanism of action has not been elucidated. Deoxynyboquinone killed cancer cells through oxidative stress and ROS formation (13, 14), and *N*-acetyl cysteine, a global free radical scavenger (13), partially blocked lethality. Here, we show that deoxynyboquinone undergoes an NQO1-dependent futile cycle similar to β-lapachone, in which O_2 is consumed, ROS is formed, and extensive DNA damage triggers PARP1 hyperactivation. Dramatic NAD$^+$/ATP pool decreases caused programmed necrosis. Deoxynyboquinone is 20- to 100-fold more potent than β-lapachone, with a significantly enhanced therapeutic window in human breast, prostate, and pancreatic cancer models *in vitro*. NQO1 processes deoxynyboquinone *in vitro* more efficiently than β-lapachone, suggesting that increased usage accounts for its enhanced potency. Significant efficacy of deoxynyboquinone at 6-fold greater potency versus β-lapachone against orthotopic Lewis lung carcinoma (LLC) is shown.

Materials and Methods

Chemicals, reagents, and antibodies

Deoxynyboquinone and β-lapachone were synthesized as described (10, 13). Streptonigrin, mitomycin C, menadione, Hoechst 33258, hydrogen peroxide (H_2O_2), cytochrome *c*,

Published OnlineFirst April 24, 2012; DOI: 10.1158/0008-5472.CAN-11-3135

propidium iodide, and dicoumarol were purchased from Sigma-Aldrich. All quinones and BAPTA-AM (Calbiochem) were dissolved in dimethyl sulfoxide (DMSO). Dihydroethidium (DHE, 5 mmol/L in DMSO) was purchased from Invitrogen Life Technologies. RH1 and α-human NQO1 antibody were provided by Dr. David Ross (University of Colorado Health Science Center, Denver, CO) and used at a 1:5,000 dilution overnight, 4°C. α-PAR (BD Pharmingen), which detects poly (ADP-ribosyl)ated (PAR) proteins (typically ADP-ribosylated PARP1), and α-PARP1 (sc-8007, Santa Cruz Biotechnology) antibodies were used at 1:4,000 and 1:2,000 dilutions, respectively. α-Tubulin was monitored for loading (15).

NQO1 enzyme assays

Deoxynyboquinone, β-lapachone, or other quinones (see Supplementary Fig. S1 for structures) were monitored as NQO1 substrates using an NADH (400 μmol/L) recycling assay and recombinant NQO1 (Sigma; ref. 10), in which NADH oxidation to NAD^+ was monitored by absorbance (A_{340} nm) and data recorded at 2 second intervals for 5 minutes. NADH oxidation rates were compared with reactions lacking β-lapachone or deoxynyboquinone, or containing dicoumarol (10 μmol/L). Initial velocities were calculated and data expressed as dicoumarol-inhibited relative units (μmol NADH oxidized/min/μmol protein; ref. 10).

O_2 consumption rates

Assays were carried out using Seahorse 24-well dishes in conjunction with an XF24 sensor cartridge and a XF24 Extracellular Flux Analyzer (Seahorse Biosciences) as per the manufacturer's instructions. Briefly, 30,000 cells per well were seeded using a 2-step process, and cells grown as above with unseeded background correction wells. O_2 consumption rates (OCR) and proton production rates were measured using the XF24 Analyzer and Assay Wizard software. Data represent means, %treated/control (T/C,%) ±SE from quadruplet assessments.

Nucleotide analyses

Changes in intracellular NAD^+ pools were measured using Fluorescent NAD/NADH Detection Kits (Cell Technology, Inc.; ref. 2). NAD^+/NADH levels were graphed as means, ±SE from at least 3 independent experiments carried out in sextuplets each. Changes in ATP *in vivo* were measured as described (2–4) and using a colorimetric/fluorometric assay (BioVision).

Immunoblotting, ROS formation

Western blots were carried out as described (3). ROS (superoxide) formation was monitored by DHE staining and microscopy. Quantitative data were analyzed using NIH ImageJ software, in which data are means, ±SE of 100 cells and duplicate experiments conducted in triplicate.

PAR formation

PAR formation *in vivo* was assessed by Western blotting controlled for α-tubulin (2–4). Chemiluminescence ELISA assays, to quantify PAR formation, were carried out by HT PARP *in vivo* Pharmacodynamic II Assays (Trevigen, Inc.). Untreated or treated cells were incubated with α−PAR antibody, then with goat α-rabbit IgG-horseradish peroxidase. Chemiluminescence by PeroxyGlow assays were expressed as means, ±SE from 3 independent experiments.

TUNEL assays

Terminal deoxynucleotidyl transferase dUTP nick end-labeling (TUNEL) assays were carried out by FC-500 flow cytometry (Beckman Coulter Electronics; ref. 10), and data were means, ±SE from 3 independent experiments, carried out in triplicate.

Cell lines and culture

Endogenous NQO1 overexpressing human A549 NSCLC, MCF-7 breast, MIA PaCa-2 pancreatic, PC-3 prostate, and HT1080 sarcoma cancer cells were obtained (3, 4, 16), MAP tested and DNA fingerprinted (ATC). $NQO1^{-}$*2 polymorphic human H596 NSCLC or MDA-MB-231 triple-negative breast, and genetically matched $NQO1^+$, cancer cells were generated by us (2, 4). $NQO1^+$ human PC-3 and genetically matched stable lentiviral short hairpin RNA (shRNA)-NQO1 knockdown, prostate cancer cells were generated by us (16). Cancer cells were grown in DMEM with 5% FBS. MDA-MB-231 cells were grown in RPMI 1640. Cells were cultured at 37°C in a 5% CO_2 95% air humidified atmosphere and were *Mycoplasma* free.

PARP1 siRNA knockdown

siRNA specific to the open reading frame of PARP1, 5′-CCAAAGGAATTCCGAGAAA-3′ (Thermo Fisher Scientific) was transiently transfected into cancer cells. PARP1 knockdown was confirmed using Western blot assays. Results were confirmed using the ON-TARGETplus PARP1 SMARTpool.

Survival

Relative survival assays were assessed as described (3) and correlated well with colony forming assays (15). Results were reported as means, ±SE from sextuplate repeats. Experiments were independently repeated 3 times.

Hepatocyte metabolic stability and pharmacokinetic assessments

During initial maximum-tolerated dose evaluations for deoxynyboquinone (10 mg/kg), pharmacokinetics for deoxynyboquinone was assessed and compared with prior β-lapachone (30 mg/kg) pharmacokinetic data (12) as described in Supplementary Material and Methods. The metabolic stability of deoxynyboquinone versus β-lapachone was examined in a standard *in vitro* hepatocyte assay (Supplementary Materials and Methods).

Deoxynyboquinone efficacy against orthotopic LLC

Antitumor efficacy. LLC cells (0.5×10^6) were intravenously injected into the tail veins of female (~22 gm) athymic nude mice. Two days later, randomized groups of mice (5 per group) were treated intravenously with hydroxypropyl-β-cyclodextrin (HPβCD) vehicle alone, or -β-lapachone (30 mg/kg) or deoxynyboquinone (2.5–10 mg/kg) dissolved in

Published OnlineFirst April 24, 2012; DOI: 10.1158/0008-5472.CAN-11-3135

HPβCD (12), every other day for 5 injections; mice treated with HPβCD (600 or 1,000 mg/kg for β-lapachone or deoxynyboquinone, respectively) did not influence tumor growth or survival. Later (18 days posttumor inoculation), mice were euthanized, lungs removed, and average lung wet weights of tumor-bearing minus control nontumor-bearing animals calculated. Lungs were visually examined to confirm LLC nodules. Tumors and associated normal lung tissue were also assessed for PARP1 hyperactivation (PAR formation) and ATP loss. Experiments were carried out twice and average lung wet weights graphed/group.

Survival. LLC-bearing mice were treated with HPβCD alone, β-Lap-HPβCD (30 mg/kg), or DNQ-HPβCD (5 mg/kg) as above and monitored for changes in weight and survival, and Kaplan-Meier curves generated. *P* values were reported with asterisks. All animal protocols have Institutional Animal Care and Use Committee approval (#2008-1080, UT Southwestern).

Statistical analyses

Student *t* tests were used to determine statistical significance from experiments repeated at least 3 independent times. *P* values were reported by asterisks as indicated.

Results

Deoxynyboquinone kills cancer cells in an NQO1-dependent manner

We examined the lethality of deoxynyboquinone with or without dicoumarol, an NQO1 inhibitor, using 2 cancer cell lines, MCF-7 (breast) and A549 (NSCLC), that endogenously express elevated NQO1 levels (Fig. 1). Deoxynyboquinone-induced lethality was compared with β-lapachone and menadione (Fig. 1A); dicoumarol prevented β-lapachone, but potentiated menadione lethality in $NQO1^+$ cells (10, 17). Dicoumarol spared deoxynyboquinone lethality in both cells (Fig. 1B). However, deoxynyboquinone was approximately 20-fold more potent than β-lapachone (compare Fig. 1B and C). As with β-lapachone (5 μmol/L), a minimum 2-hour exposure of A549 cells to deoxynyboquinone (0.25 μmol/L) was required for complete lethality (Supplementary Fig. S2A) and extensive DNA base damage and SSBs (Supplementary Fig. S2B). This dose was used in all subsequent studies.

Deoxynyboquinone was processed *in vitro* at a significantly increased rate relative to β-lapachone, or other quinones (streptonigrin, menadione, RH1, and mitomycin C). At 1 μmol/L, deoxynyboquinone was reduced by NQO1 approximately 13-fold more efficiently than other quinones (Supplementary Table S1, Supplementary Fig. S1). Importantly, at LD_{100} levels (0.25 μmol/L for deoxynyboquinone, 5 μmol/L for β-lapachone) in A549 cells, the NQO1 NADH recycling activities *in vitro* using deoxynyboquinone or β-lapachone were essentially identical (Supplementary Table S2), suggesting that the catalytic efficiency of NQO1 for deoxynyboquinone was at least 20-fold greater than for β-lapachone. Menadione was a significantly (>20-fold) less efficient substrate *in vitro* for NQO1 at its LD_{90}, as reported (10). Dicoumarol potentiated menadione lethality in MCF-7 cells, but not in A549 cells (Fig. 1D).

Deoxynyboquinone efficiently kills a wide spectrum of cancer cells in an NQO1-dependent manner

Deoxynyboquinone efficiently killed human MIA PaCa-2 pancreatic (Fig. 2A) and HT1080 sarcoma cancer cells (Fig. 2B) with LD_{50} values of 48 and 178 nmol/L, respectively; deoxynyboquinone showed greater potency in pancreatic cells, in general. Dicoumarol protected both cells. We then treated genetically matched $NQO1^+$ versus $NQO1^-$ human H596 NSCLC or MDA-MB-231 breast cancer cells with deoxynyboquinone; *2 $NQO1^-$ polymorphic H596 and MDA-MB-231 cells were separately corrected for NQO1 expression as clones or pooled populations (4, 10). Deoxynyboquinone killed all $NQO1^+$ clones and pooled populations, but not genetically matched $NQO1^-$ cells (Fig. 2C and D). Similarly, human PC-3 cells stably knocked down for NQO1 expression (shNQ) were spared versus $NQO1^+$ PC-3 cells expressing nonsilencing shRNA (Fig. 2E). Deoxynyboquinone-induced cytotoxicity in nonsilenced $NQO1^+$ PC-3 cells was prevented by dicoumarol (Fig. 2E), as in parental PC-3 cells. PC-3 cells treated with dicoumarol were similarly spared from deoxynyboquinone lethality as were stable NQO1 knockdown shNQ PC-3 cells (Fig. 2E). Colony forming assays confirmed the NQO1 dependency of deoxynyboquinone (Fig. 2F). LD_{50} values for deoxynyboquinone versus β-lapachone cytotoxicities in various cancers are listed in Supplementary Table S3, highlighting the NQO1-dependent potency of deoxynyboquinone.

Deoxynyboquinone NQO1-dependent lethality involves a futile cycle generating ROS

β-Lapachone-induced lethality involves a futile cycle mediated by NQO1, in which approximately 60 moles of NAD(P)H are used, forming approximately 120 moles superoxide (O_2^-) per mole β-lapachone in 2 minutes (10). We compared OCR in A549 NSCLC cells after deoxynyboquinone versus β-lapachone treatments. As with β-lapachone (Fig. 3A), deoxynyboquinone-treated A549 cells (Fig. 3B) showed dramatic OCR increases that were dose dependent and reached peak levels in 30 minutes at LD_{50} levels (Fig. 3C and D). Minimal differences between β-lapachone and deoxynyboquinone were noted, except that significantly lower deoxynyboquinone doses were needed (Fig. 3B). Dicoumarol blocked OCR from either deoxynyboquinone- or β-lapachone-treated cells, strongly suggesting that O_2 consumption was NQO1 mediated. Similar OCR increases were noted in $NQO1^+$, but not in $NQO1^-$, H596 cells (Supplementary Fig. 3A and B). Low, but detectable, O_2 consumption in $NQO1^+$ A549 cells after cotreatment of β-lapachone and dicoumarol (Fig. 3A and C) may be due to one-electron oxidoreductases (b5R and p450R) metabolizing β-lapachone. Interestingly, such OCRs with dicoumarol were not noted with deoxynyboquinone, suggesting that deoxynyboquinone was not as good a substrate for one-electron oxidoreductases (Fig. 3B and D).

We then monitored superoxide (O_2^-) formation using DHE staining. Deoxynyboquinone (0.25 μmol/L) induced dramatic ROS formation in 60 minutes in A549 cells that was prevented by dicoumarol (Fig. 3E). Exogenous catalase (CAT, 1,000 U) partially rescued deoxynyboquinone cytotoxicity (Fig. 3F). Thus, NQO1-dependent deoxynyboquinone metabolism

Published OnlineFirst April 24, 2012; DOI: 10.1158/0008-5472.CAN-11-3135

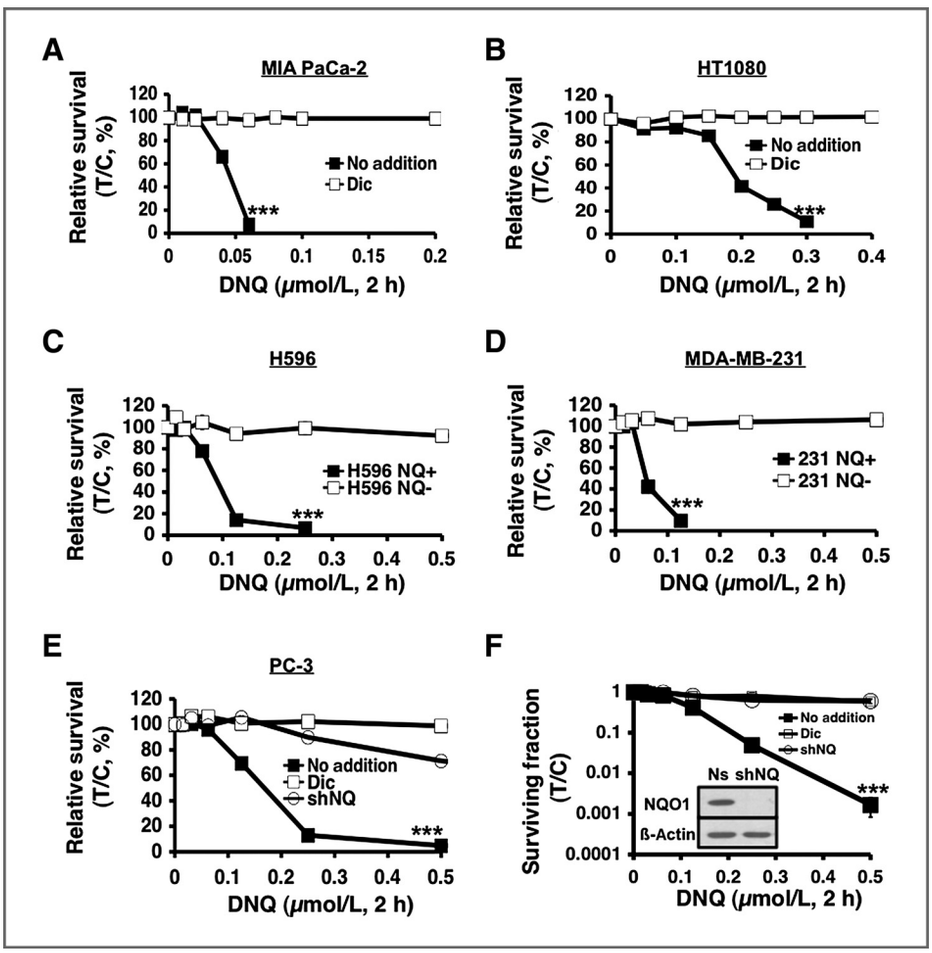

Figure 2. NQO1-dependent, deoxynyboquinone-induced lethality in various cancer cells. Deoxynyboquinone killed human MIA PaCa-2 pancreatic (A) and HT1080 sarcoma (B) cells with lethal doses of 6 and 300 nmol/L, respectively, and dicoumarol rescued lethality. NQO1- H596 NSCLC (C) or MDA-MB-231 breast cancer (D) cells were resistant to deoxynyboquinone. Exogenous overexpression of NQO1 enhanced deoxynyboquinone lethality. E, human PC-3 prostate cancer cells knocked down for NQO1 expression using shRNA-NQO1 (shNQ) were resistant to deoxynyboquinone (μmol/L, 2 hours). PC-3 cells containing nonsilencing shRNA (no addition) were sensitive to deoxynyboquinone, whereas dicoumarol suppressed lethality similar to shNQ PC-3 cells. F, clonogenic assays confirmed deoxynyboquinone lethality in $NQO1^+$ shRNA-nonsilenced Ns PC-3 cells, whereas resistance was noted in shNQ PC-3 cells, or in Ns PC-3 cells + dicoumarol. All treatments were as in E. No addition, DMSO alone as in Fig. 1. Inset, Western blot shows NQO1 knockdown, with 26 ±10 units (Supplementary Table S1). ***, $P \leq 0.001$. Dic, dicoumarol; DNQ, deoxynyboquinone.

resulted in extensive OCR, O_2^- formation, and long-lived H_2O_2 production similar to β-lapachone (2), but at 20-fold lower concentrations.

Deoxynyboquinone induces PARP1 hyperactivation, loss of essential nucleotides

Deoxynyboquinone-treated A549 cells were examined for poly(ADP-ribosyl)ated protein (PAR) formation using an ELISA method, in which peak levels were noted at approximately 10 minutes (Fig. 4A). PAR-PARP1 (PAR) formation was confirmed by Western blot analyses with similar kinetics, lasting approximately 20 minutes (Fig. 4B). Dicoumarol effectively suppressed PAR formation and blocked PARP1 hyperactivation in deoxynyboquinone-treated A549 cells (Fig. 4A). PARP1 hyperactivation induced by deoxynyboquinone in A549 cells was accompanied by dramatic NAD^+ and ATP losses. Both dose–response and time–course studies showed that NAD^+ and ATP were rapidly and extensively depleted (Figs. 4C–F), and a 2-hour exposure was sufficient for near complete NAD^+ loss in deoxynyboquinone-exposed cells (0.25 μmol/L, 2 hours, Fig. 4C and E). Dramatic ATP loss followed NAD^+ depletion in both dose- and time-dependent manners (Fig. 4D and F) that were prevented by dicoumarol. Deoxynyboquinone-induced ATP losses occurred in an NQO1-dependent manner in $NQO1^+$, but not in $NQO1^-$, H596 cells (Supplementary Fig. 4A and B).

Both PARP1 and Ca^{2+} play pivotal roles in deoxynyboquinone-induced cell death

We then transiently knocked down PARP1 using specific siRNA, which did not affect NQO1 expression (Fig. 5A). PARP1 knockdown significantly prevented NAD^+ (Fig. 5B) and ATP losses (Supplementary Fig. S5) in deoxynyboquinone-exposed A549 cells versus parental or nontargeting siRNA-treated (siNT) cells. Transient PARP1 knockdown significantly decreased programmed necrosis ($TUNEL^+$) 24 hours after treatment with either LD_{50} (0.125 μmol/L) or lethal (0.25 μmol/L) deoxynyboquinone doses (Fig. 5C and D), similar to effects noted with β-lapachone (2). Dicoumarol spared parental and PARP1 knockdown cells (Fig. 5D).

PARP1 hyperactivation required endoplasmic reticulum Ca^{2+} release as BAPTA-AM, an endogenous cytosolic Ca^{2+} chelator, spared β-lapachone-induced lethality (2). BAPTA-AM pretreatment significantly spared deoxynyboquinone-induced lethality in $NQO1^+$ A549 or H596 NSCLC cells using long-term survival assays (Fig. 5E, Supplementary Fig. S6), and significantly suppressed PARP1 hyperactivation, noted by abrogation of NAD^+ depletion (no addition vs. BAPTA-AM, Fig. 5F).

Published OnlineFirst April 24, 2012; DOI: 10.1158/0008-5472.CAN-11-3135

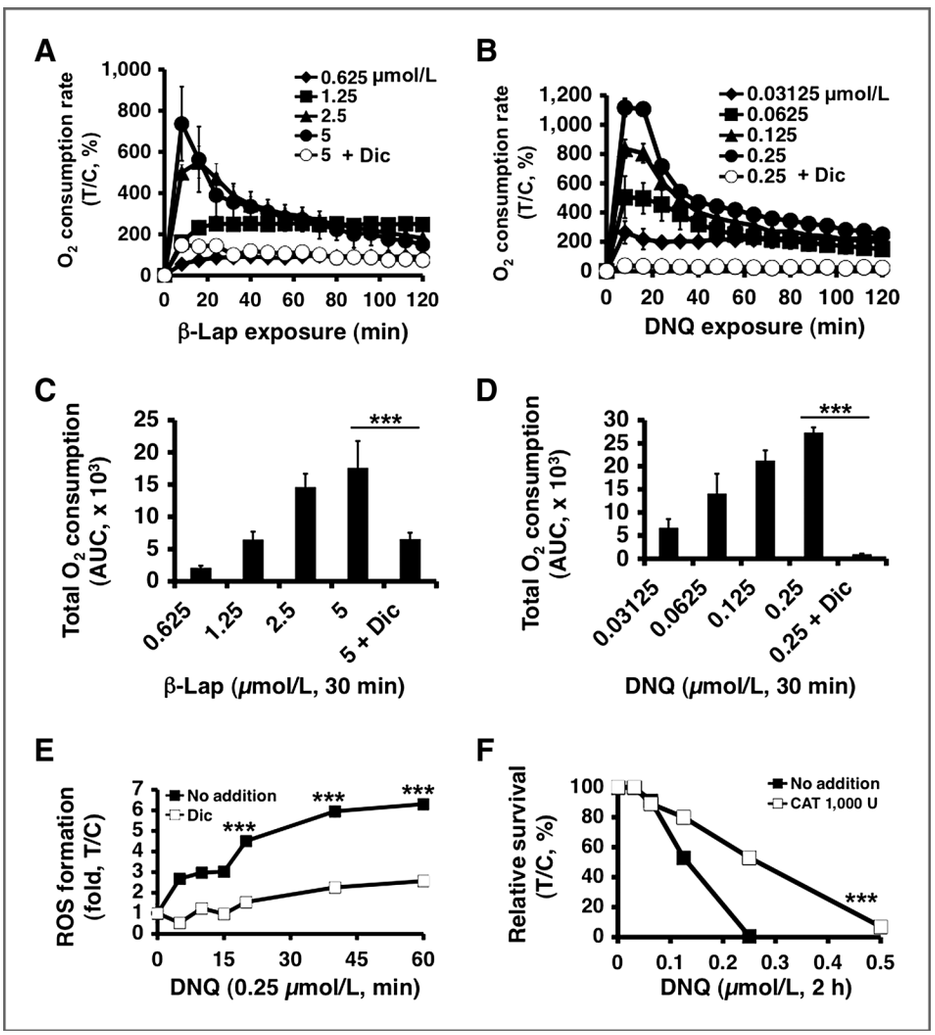

Figure 3. Elevated ROS in deoxynyboquinone-treated endogenous NQO1$^+$ cancer cells. A, OCR in A549 cells treated with or without β-lapachone ± dicoumarol (40 μmol/L) were monitored at 8-minute intervals for 2 hours. Data were means, ±SE normalized to untreated controls. Experiments were done 3 times in quadruplet. B, OCRs were measured after deoxynyboquinone treatment. Experiments were carried out as in A. Quantitative data of total OCR 30 minutes after β-lapachone (C) or deoxynyboquinone (D) treatments at different doses. Data from A and B were used. E, A549 cells were treated with or without deoxynyboquinone (0.25 μmol/L) ± dicoumarol (40 μmol/L). ROS formation was assessed by DHE staining. Results are means, ±SE of arbitrary units (13) measured by staining intensity from ≥100 cells using NIH Image J. F, deoxynyboquinone (μmol/L, 2 hours) -exposed A549 cells were cotreated with ± catalase (CAT, 1,000 U) and clonogenic survival monitored. ***, $P \leq 0.001$, comparing deoxynyboquinone treated A549 cells ± catalase cotreatment. Dic, dicoumarol; DNQ, deoxynyboquinone; β-lap, β-lapachone.

Potential NQO1-dependent therapeutic window of deoxynyboquinone

Differential NQO1 expression in various solid tumors versus normal tissue can be effectively exploited using β-lapachone, resulting in a wide therapeutic window *in vitro* (4) that predicted its antitumor efficacy *in vivo* (3, 16). A549 cells were exposed to various deoxynyboquinone doses, with or without dicoumarol (40 μmol/L), at various times to assess the long-term survival "potential therapeutic window," as done with β-lapachone in NSCLC, pancreatic, and prostate cancers (3, 12, 16). In A549 cells, deoxynyboquinone exhibited a much broader therapeutic window than β-lapachone (compare Figs. 6A–J to those in ref. 4). Deoxynyboquinone-treated (0.25 μmol/L) A549 cells were rescued by dicoumarol (Fig. 6A–H). However, as the length of deoxynyboquinone exposure was increased to more than 24 hours, only approximately 70% of the cells were spared by dicoumarol (Fig. 6I). Lethality was further increased after more than 48 hours of deoxynyboquinone exposure in cells treated with dicoumarol (Fig. 6J), with limited lethality increases in parental NQO1$^+$ cells (compare solid square lines at 2 vs. 24 hours, Fig. 6C and H, respectively). Similar responses were noted in NQO1$^+$ vs. NQO1$^-$ H596 cells (Supplementary Fig. S7A–C).

Deoxynyboquinone antitumor efficacy

Using an extremely aggressive orthotopic LLC model in athymic mice, we examined the antitumor efficacy of deoxynyboquinone (Fig. 7); murine LLC tumors have approximately 80 U of NQO1 activity versus less than 100 U in mouse normal lungs. Mice were treated every other day for 5 injections with HPβCD alone, deoxynyboquinone (2.5, 5, and 10 mg/kg) or β-lapachone (30 mg/kg). Later (18 days), lungs were removed, weighed, and visually scored for tumor nodules (Fig. 7A and B). DNQ-HPβCD (5 and 10 mg/kg) or β-Lap-HPβCD–treated mice showed significant tumor growth reductions, confirmed by decreases in tumor nodule formation and histology (Fig. 7A and B). No long-term pathologic effects (monitored 18 days after one regimen) of deoxynyboquinone or β-lapachone were noted in liver (Fig. 7C), lung, bone marrow, spleen, or thymus; unlike humans, mice have relatively high liver NQO1 levels. Overall survival confirmed significant antitumor efficacy of deoxynyboquinone (at 5 mg/kg; $P \leq 0.04$), at a 6-fold lower dose

Published OnlineFirst April 24, 2012; DOI: 10.1158/0008-5472.CAN-11-3135

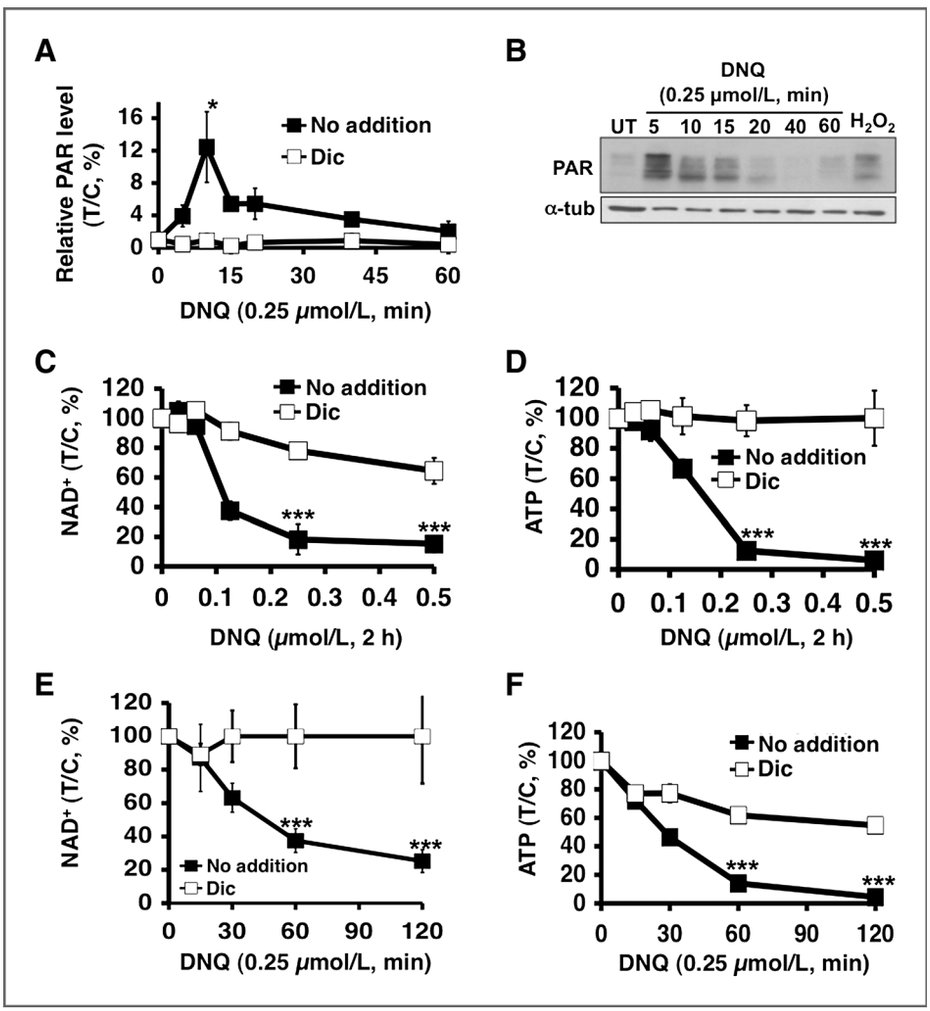

Figure 4. Deoxynyboquinone induces NQO1-dependent PARP1 hyperactivation and nucleotide depletion. A, PARP1 hyperactivation, monitored by poly (ADP)-ribosylated protein (PAR) formation using an ELISA method, was detected in A549 cells treated with or without deoxynyboquinone, ± dicoumarol (40 μmol/L). Data are means, ±SE from 3 independent experiments. B, Western blot assays confirmed PAR formation (PAR-PARP1, ~120 kDa) in A549 cells treated with or without 0.25 μmol/L deoxynyboquinone at indicated times (minutes). Cells were treated with H_2O_2 (1 mmol/L, 15 minutes) as a positive control for PAR formation (PAR). Loading was controlled by α-tubulin levels. Dose-dependent NAD^+ (C) and ATP (D) loss in A549 cells after various deoxynyboquinone doses ± dicoumarol (40 μmol/L). NAD^+ (E) and ATP (F) depletion was analyzed at indicated times, with or without deoxynyboquinone (0.25 μmol/L) ± dicoumarol (40 μmol/L). Data are means, ±SE from 3 independent experiments, in triplicate. *, $P \leq 0.05$; ***, $P \leq 0.001$. DNQ, deoxynyboquinone; α-tub, α-tubulin.

than β-lapachone (30 mg/kg; Fig. 7D). Finally, PAR formation and energy (ATP) losses in LLC tumors after deoxynyboquinone or β-lapachone exposures confirmed their PARP1 hyperactivation-mediated programmed necrotic mechanism (Fig. 7E and F); tumor-specific ATP losses were confirmed by LC/MS/MS analyses. In contrast, associated normal lung tissue was unaffected, showing no PARP1 hyperactivation or ATP loss (Fig. 7E and F).

Metabolic stability measurements using murine hepatocytes and plasma pharmacokinetic analyses revealed greater metabolic stability and prolonged plasma half-life of deoxynyboquinone versus β-lapachone (Supplementary Fig. S8A and B and Supplementary Table S4).

Discussion

Identifying exploitable differences between cancerous and healthy tissue is critical for development of next-generation cancer treatments. NQO1 is overexpressed in a majority of solid tumors, in angiogenic and bone marrow endothelial cells (18, 19), and is induced by exposure to certain quinones (20) or ionizing radiation (21, 22). NQO1 overexpression in solid tumor versus associated normal tissue was reported in approximately 80% NSCLC tumors at 20- to 40-fold (4), approximately 70% breast tumors at 10- to 20-fold (23), approximately 90% pancreatic tumors at 20- to 30-fold (24), approximately 60% prostate tumors at 10- to 20-fold (3), and approximately 60% colon tumors at 5- to 10-fold (25). Thus, compounds "bioactivated" by NQO1 have potential for "personalized" anticancer therapy.

β-Lapachone and deoxynyboquinone kill cancer cells through the same NQO1-dependent programmed necrotic (necroptosis) pathway. At minimally lethal doses of each agent (0.25 μmol/L for deoxynyboquinone, 5 μmol/L for β-lapachone), a minimum exposure time (2 hours) was noted for 100% lethality *in vitro*; H_2O_2 was the apparent obligatory ROS intermediate required for PARP1 hyperactivation and lethality, as catalase prevented both; Ca^{2+} release (2, 26) for PARP1 hyperactivation and lethality was required, as BAPTA-AM prevented both; PARP1 hyperactivation caused dramatic ATP and NAD^+ losses; and cells were killed in the same time frame and with unique proteolysis (e.g., atypical PARP1 and p53 cleavage). Understanding this mechanism will lead to further improvement in their efficacy.

Published OnlineFirst April 24, 2012; DOI: 10.1158/0008-5472.CAN-11-3135

The potency and NQO1-dependent therapeutic window (Fig. 6) of deoxynyboquinone and its apparent reduced metabolism by one-electron oxidoreductases, make this drug (or derivatives) very promising. We elucidated its mechanism of action in various cancer cells, showing that it induced programmed necrosis identical to β-lapachone, but with approximately 20-fold increased potency. NQO1$^+$ cells were selectively hypersensitive to deoxynyboquinone, whereas genetically matched NQO1$^-$ cells were resistant. NQO1$^+$ cells were rescued from deoxynyboquinone-induced cytotoxicity by NQO1 knockdown or by chemical inhibition (via DIC) of NQO1. Exposure of NQO1$^+$ cancer cells to deoxynyboquinone elicited elevated superoxide levels, with concomitant and significant OCR. Downstream, deoxynyboquinone stimulated PARP1 hyperactivation in a mechanism essentially identical to β-lapachone, which correlated well with NAD$^+$/ATP losses, and NADH recycling assays confirmed futile cycling of deoxynyboquinone by NQO1.

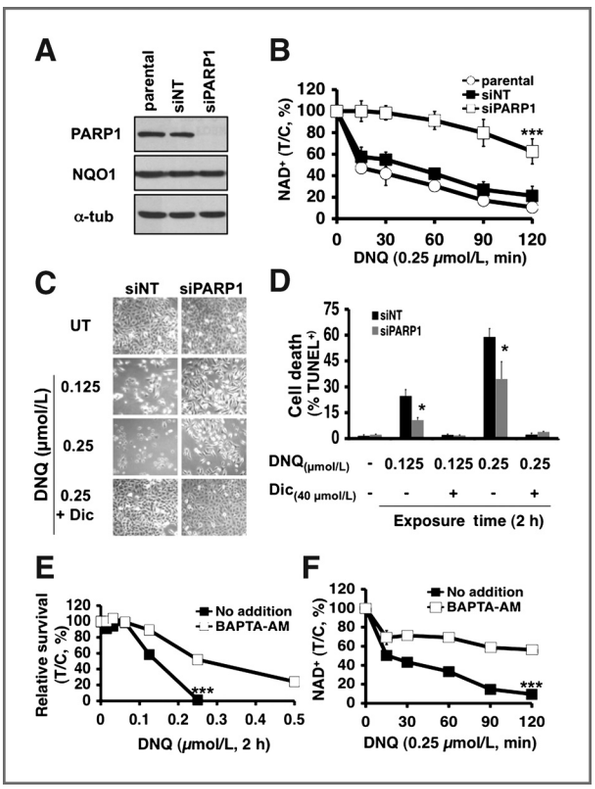

Figure 5. PARP1 and Ca^{2+} play pivotal roles in deoxynyboquinone-induced lethality. A, steady-state PARP1, NQO1, and α-tubulin levels were assessed by Western blots in mock-transfected, transiently PARP1 knockdown (siPARP1) or nontargeted siRNA (siNT) cells 48 hours posttransfection. Loading was monitored by α-tubulin levels. B, PARP1 is essential for NAD$^+$ loss at the indicated times (minutes) in deoxynyboquinone-treated (0.25 μmol/L) NQO1$^+$ A549 cells. *P* values compare NAD$^+$ levels in PARP1 knockdown versus parental or siNT A549 cells. C, micrographs of deoxynyboquinone-treated nontargeted (siNT) or PARP1-specific (siPARP1) siRNA knockdown A549 cells at 24 hours posttreatment with LD_{50} or lethal doses, ± dicoumarol (40 μmol/L). D, PARP1 knockdown significantly protected A549 cells from deoxynyboquinone-induced programmed necrosis (%TUNEL+ cells). Treatment conditions were as in C. Data are means, ±SE from 3 independent experiments. E, long-term survival of A549 cells pretreated or not with BAPTA-AM (5 μmol/L, 60 minutes), with or without a 2-hour deoxynyboquinone pulse. F, BAPTA-AM pretreatment of deoxynyboquinone-exposed A549 cells prevented NAD$^+$ loss. *, $P \leq 0.05$; ***, $P \leq 0.001$. DNQ, deoxynyboquinone; α-tub, α-tubulin.

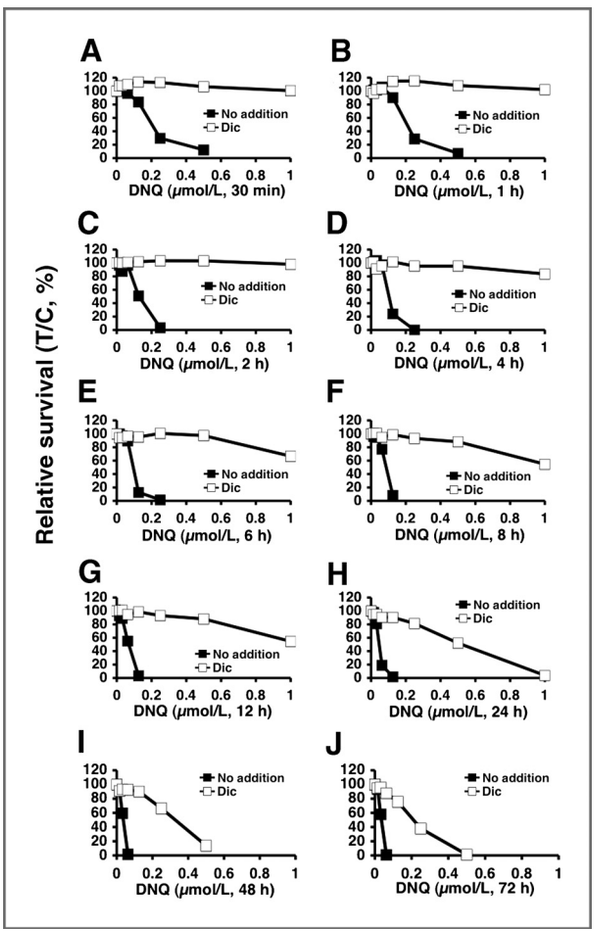

Figure 6. Deoxynyboquinone shows a broad NQO1-dependent therapeutic window. Relative survival was monitored in A549 cells treated with various deoxynyboquinone concentrations (μmol/L) ± dicoumarol (40 μmol/L) for 30 minutes (A), 1 hour (B), 2 hours (C), 4 hours (D), 6 hours (E), 8 hours (F), 12 hours (G), 24 hours (H), 48 hours (I), and 72 hours (J). Graphed are means, ±SE of duplicate experiments, repeated in sextuplets. DNQ, deoxynyboquinone.

Deoxynyboquinone has an apparently broader NQO1-dependent therapeutic window *in vitro* (Fig. 6) than β-lapachone (4) using A549 cells as a surrogate. Similar data were obtained using NQO1$^+$ versus NQO1$^-$ H596 cells (Supplementary Fig. S7). Thus, deoxynyboquinone may not be as good a substrate as β-lapachone for p450R and b5R, as β-lapachone-treated cells consumed low, but detectable O_2 even with DIC, whereas OCR was blocked in deoxynyboquinone-treated cells (Figs. 3C and D). Antitumor (Fig. 7), pharmacokinetic and metabolic stability (Supplementary Material, Table S4 and Supplementary Fig. S8A and B) data support a strong antitumor efficacy potential for deoxynyboquinone, with increased metabolic stability in intact hepatocytes *in vitro* and a longer half-life than β-lapachone. The increased metabolic stability of deoxynyboquinone

Published OnlineFirst April 24, 2012; DOI: 10.1158/0008-5472.CAN-11-3135

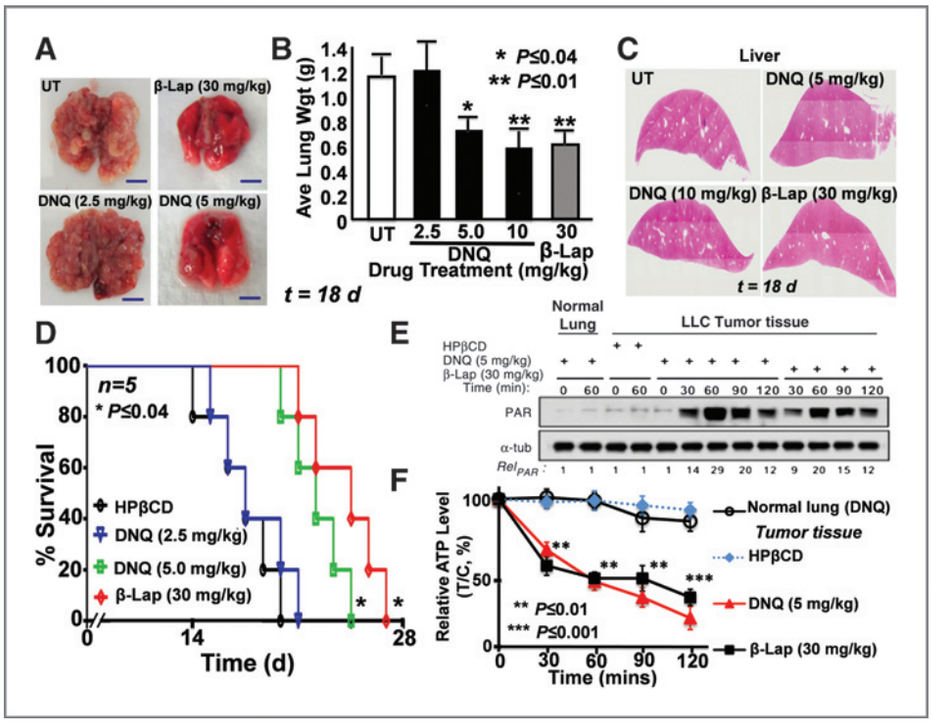

Figure 7. Deoxynyboquinone shows equivalent efficacy to β-lapachone at a 6-fold lower dose. In A–C, mice bearing visible tumors were treated once every other day for 5 injections as in the text, and average wet weight tumor volumes assessed (A and B). Tumor nodules were confirmed visually (A) and histologically (not shown), and average wet weights calculated (B). DNQ-HPβCD (5 or 10 mg/kg) or β-Lap-HPβCD (30 mg/kg) caused tumor weight decreases that were equivalent ($P > 0.6$). Normal tissues were assessed with no long-term pathologic injury noted; see H&E-stained livers (C). D, Kaplan-Meier survival curves showed significant ($P \leq 0.04$) survival advantages of deoxynyboquinone (5 mg/kg) or β-lapachone-treated (30 mg/kg) groups. Groups were HPβCD alone (1,000 mg/kg), deoxynyboquinone (2.5, 5.0 mg/kg), or β-lapachone (30 mg/kg) in HPβCD. *, $P \leq 0.04$; **, $P \leq 0.01$. In E and F, PAR formation and ATP loss confirmed programmed necrotic mechanism of deoxynyboquinone- or β-lapachone–treated LLC tumors where animals were treated as in A–C with 3 doses and 24 hours later lungs were removed. Note the lack of response of associated normal lung tissue. **, $P < 0.01$; ***, $P < 0.001$; α-tub, α-tubulin; and PAR, PAR-PARP1. DNQ, deoxynyboquinone; β-lap, β-lapachone.

is consistent with a lower affinity for one-electron oxidoreductases (i.e., b5R and P450R), as these enzymes are elevated in mouse liver. Deoxynyboquinone showed equivalent antitumor activity, suppressed tumor growth, and increased survival of tumor-bearing mice as β-lapachone, but at 6-fold lower doses (Fig. 7), consistent with its therapeutic window *in vitro* (Fig. 6). However, our studies *in vivo* are in no way an optimization of deoxynyboquinone delivery. Significant dose-limiting methemaglobinemia was noted in deoxynyboquinone-treated mice, and much less with β-lapachone (12). Such blood-borne toxicity can be easily resolved, however, as methemaglobinemia was completely prevented using β-lapachone "stealth" micellar delivery (12). In addition, novel deoxynyboquinone analogs that we believe will avoid such limiting toxicities are currently being tested using orthotopic breast, lung, prostate, and pancreatic tumor models.

Our comparison of deoxynyboquinone to various quinones as NQO1 substrates *in vitro* using NADH reutilization assays (10) may explain its increased potency. At 1 μmol/L, NQO1 processed deoxynyboquinone approximately 13-fold more efficiently than β-lapachone (1,400 ± 80 vs. 110 ± 20 relative units, Supplementary Table S1). At equitoxic (LD_{100}) levels, similar NQO1 enzymatic activities (680 ± 110 vs. 530 ± 60 relative units for 5 μmol/L β-lapachone vs. 0.25 μmol/L deoxynyboquinone, respectively, Supplementary Table S2) were noted. The potential therapeutic window of deoxynyboquinone seems superior to β-lapachone, making deoxynyboquinone a potentially safer candidate for use as a chemotherapeutic drug, although increased potency may translate into greater normal tissue toxicity. Thus, our studies strongly suggest that deoxynyboquinone and future more soluble derivatives and/or stealth polymeric nanoparticles will be very promising anticancer therapeutics for the treatment of NSCLC, pancreatic, and breast cancers.

Disclosure of Potential Conflicts of Interest

P.J. Hergenrother, J. Gao, and D.A. Boothman are consultants for StemPAR Sciences, Inc., which licensed patents from UT Southwestern and University of Illinois at Urbana-Champaign. No potential conflicts of interest were disclosed by the other authors.

Authors' Contributions

Conception and design: X. Huang, Y. Dong, E.A. Bey, P.J. Hergenrother, D.A. Boothman

Development of methodology: X. Huang, Y. Dong, E.A. Bey, M. Patel, Y. Wang, J. Gao, P.J. Hergenrother, D.A. Boothman

Acquisition of data (provided animals, acquired and managed patients, provided facilities, etc.): X. Huang, Y. Dong, J.A. Kilgore, L.-S. Li, E.I. Parkinson, Y. Wang, D.A. Boothman

Analysis and interpretation of data (e.g., statistical analysis, biostatistics, computational analysis): X. Huang, Y. Dong, E.A. Bey, J.A. Kilgore, J.S. Bair, L.-S. Li, M. Patel, E. Parkinson, Y. Wang, N.S. Williams, P.J. Hergenrother, D.A. Boothman
Writing, review, and/or revision of the manuscript: X. Huang, Y. Dong, E.A. Bey, J.A. Kilgore, J.S. Bair, L.-S. Li, E.I. Parkinson, N.S. Williams, P.J. Hergenrother, D.A. Boothman
Administrative, technical, or material support (i.e., reporting or organizing data, constructing databases): X. Huang, Y. Dong, L.-S. Li, M. Patel, E.I. Parkinson, P.J. Hergenrother, D.A. Boothman
Study supervision: L.-S. Li, N.S. Williams, P.J. Hergenrother, D.A. Boothman

Acknowledgments

The authors thank Dr. William G. Bornmann (MD Anderson) for supplying β-lapachone and the Imaging and Chemistry and Cancer Shared Resources, SCC.

Grant Support

This work was supported by NIH/NCI grant CA102792 to D.A. Boothman and separate support from the University of Illinois. This work was also supported by an AACR Innovator Award, PanCan Block Foundation grant to D.A. Boothman.

The costs of publication of this article were defrayed in part by the payment of page charges. This article must therefore be hereby marked *advertisement* in accordance with 18 U.S.C. Section 1734 solely to indicate this fact.

Received September 21, 2011; revised April 13, 2012; accepted April 16, 2012; published OnlineFirst April 24, 2012.

References

1. Pavet V, Portal MM, Moulin JC, Herbrecht R, Gronemeyer H. Towards novel paradigms for cancer therapy. Oncogene 2011;30:1–20.
2. Bentle MS, Reinicke KE, Bey EA, Spitz DR, Boothman DA. Calcium-dependent modulation of poly(ADP-ribose) polymerase-1 alters cellular metabolism and DNA repair. J Biol Chem 2006;281:33684–96.
3. Dong Y, Bey EA, Li LS, Kabbani W, Yan J, Xie XJ, et al. Prostate cancer radiosensitization through poly(ADP-Ribose) polymerase-1 hyperactivation. Cancer Res 2010;70:8088–96.
4. Bey EA, Bentle MS, Reinicke KE, Dong Y, Yang CR, Girard L, et al. An NQO1- and PARP1-mediated cell death pathway induced in non-small-cell lung cancer cells by beta-lapachone. Proc Natl Acad Sci U S A 2007;104:11832–7.
5. Ross D, Siegel D. NAD(P)H:quinone oxidoreductase 1 (NQO1, DT-diaphorase), functions and pharmacogenetics. Methods Enzymol 2004;382:115–44.
6. Danson S, Ward TH, Butler J, Ranson M. DT-diaphorase: a target for new anticancer drugs. Cancer Treat Rev 2004;30:437–49.
7. McKeown SR, Cowen RL, Williams KJ. Bioreductive drugs: from concept to clinic. Clin Oncol (R Coll Radiol) 2007;19:427–42.
8. Winski SL, Hargreaves RH, Butler J, Ross D. A new screening system for NAD(P)H:quinone oxidoreductase (NQO1)-directed antitumor quinones: identification of a new aziridinylbenzoquinone, RH1, as a NQO1-directed antitumor agent. Clin Cancer Res 1998;4:3083–8.
9. Curt GA, Kelley JA, Kufta CV, Smith BH, Kornblith PL, Young RC, et al. Phase II and pharmacokinetic study of aziridinylbenzoquinone [2,5-diaziridinyl-3,6-bis(carboethoxyamino)-1,4-benzoquinone, diaziquone, NSC 182986] in high-grade gliomas. Cancer Res 1983;43:6102–5.
10. Pink JJ, Planchon SM, Tagliarino C, Varnes ME, Siegel D, Boothman DA. NAD(P)H:Quinone oxidoreductase activity is the principal determinant of beta-lapachone cytotoxicity. J Biol Chem 2000;275:5416–24.
11. Reinicke KE, Bey EA, Bentle MS, Pink JJ, Ingalls ST, Hoppel CL, et al. Development of beta-lapachone prodrugs for therapy against human cancer cells with elevated NAD(P)H:quinone oxidoreductase 1 levels. Clin Cancer Res 2005;11:3055–64.
12. Blanco E, Bey EA, Khemtong C, Yang SG, Setti-Guthi J, Chen H, et al. Beta-lapachone micellar nanotherapeutics for non-small cell lung cancer therapy. Cancer Res 2010;70:3896–904.
13. Bair JS, Palchaudhuri R, Hergenrother PJ. Chemistry and biology of deoxynyboquinone, a potent inducer of cancer cell death. J Am Chem Soc 2010;132:5469–78.
14. Tudor G, Gutierrez P, Aguilera-Gutierrez A, Sausville EA. Cytotoxicity and apoptosis of benzoquinones: redox cycling, cytochrome c release, and BAD protein expression. Biochem Pharmacol 2003;65:1061–75.
15. Wuerzberger SM, Pink JJ, Planchon SM, Byers KL, Bornmann WG, Boothman DA. Induction of apoptosis in MCF-7:WS8 breast cancer cells by beta-lapachone. Cancer Res 1998;58:1876–85.
16. Li LS, Bey EA, Dong Y, Meng J, Patra B, Yan J, et al. Modulating endogenous NQO1 levels identifies key regulatory mechanisms of action of beta-lapachone for pancreatic cancer therapy. Clin Cancer Res 2011;17:275–85.
17. Criddle DN, Gillies S, Baumgartner-Wilson HK, Jaffar M, Chinje EC, Passmore S, et al. Menadione-induced reactive oxygen species generation via redox cycling promotes apoptosis of murine pancreatic acinar cells. J Biol Chem 2006;281:40485–92.
18. Siegel D, Franklin WA, Ross D. Immunohistochemical detection of NAD(P)H:quinone oxidoreductase in human lung and lung tumors. Clin Cancer Res 1998;4:2065–70.
19. Siegel D, Ryder J, Ross D. NAD(P)H: quinone oxidoreductase 1 expression in human bone marrow endothelial cells. Toxicol Lett 2001;125:93–8.
20. Begleiter A, Fourie J. Induction of NQO1 in cancer cells. Methods Enzymol 2004;382:320–51.
21. Boothman DA, Meyers M, Fukunaga N, Lee SW. Isolation of x-ray-inducible transcripts from radioresistant human melanoma cells. Proc Natl Acad Sci U S A 1993;90:7200–4.
22. Choi EK, Terai K, Ji IM, Kook YH, Park KH, Oh ET, et al. Upregulation of NAD(P)H:quinone oxidoreductase by radiation potentiates the effect of bioreductive beta-lapachone on cancer cells. Neoplasia 2007;9:634–42.
23. Marin A, Lopez de Cerain A, Hamilton E, Lewis AD, Martinez-Penuela JM, Idoate MA, et al. DT-diaphorase and cytochrome B5 reductase in human lung and breast tumours. Br J Cancer 1997;76:923–9.
24. Lewis AM, Ough M, Hinkhouse MM, Tsao MS, Oberley LW, Cullen JJ. Targeting NAD(P)H:quinone oxidoreductase (NQO1) in pancreatic cancer. Mol Carcinogenesis 2005;43:215–24.
25. Mikami K, Naito M, Ishiguro T, Yano H, Tomida A, Yamada T, et al. Immunological quantitation of DT-diaphorase in carcinoma cell lines and clinical colon cancers: advanced tumors express greater levels of DT-diaphorase. Jpn J Cancer Res 1998;89:910–5.
26. Tagliarino C, Pink JJ, Dubyak GR, Nieminen AL, Boothman DA. Calcium is a key signaling molecule in beta-lapachone-mediated cell death. J Biol Chem 2001;276:19150–9.

Cancer Research
The Journal of Cancer Research (1916–1930) | The American Journal of Cancer (1931–1940)

AACR American Association for Cancer Research

An NQO1 Substrate with Potent Antitumor Activity That Selectively Kills by PARP1-Induced Programmed Necrosis

Xiumei Huang, Ying Dong, Erik A. Bey, et al.

Cancer Res 2012;72:3038-3047. Published OnlineFirst April 24, 2012.